78-93

Thermal Stresses in a Plasma-Sprayed Ceramic Gas Path Seal

Christopher M. Taylor* and Robert C. Bill†
NASA Lewis Research Center, Cleveland, Ohio

A ceramic/metallic aircraft gas turbine outer gas path seal designed to enable improved engine performance is studied. Transient temperature and stress profiles in a test seal geometry have been determined by numerical analysis. During a simulated engine deceleration cycle from sea-level takeoff to idle conditions, it has been shown that the maximum seal temperature occurs below the seal surface and that the top layer of the seal is probably subjected to tensile stresses exceeding the modulus of rupture. In this regard the analysis supports experimental thermal fatigue testing of the seal where surface cracking has been observed. In the stress analysis both two- and three-dimensional finite element computer programs were used. Predicted trends of the simpler and more easily usable two-dimensional element programs were borne out by the three-dimensional finite element program results.

Introduction

IMPROVED gas turbine efficiencies can be realized through a variety of approaches, including increased turbine inlet temperatures and the maintaining of induced turbine blade tip clearances. The high-pressure turbine (HPT) outer gas path seal system, an example of which is shown in Fig. 1, is an important feature from the standpoint of engine performance. Its primary function is to maintain minimum clearance over the blade tip, thereby reducing aerodynamic and leakage losses. For example, in a typical large commercial aircraft gas turbine engine, it is estimated that for every 0.010-in. reduction in HPT tip clearance realized, a performance payoff of 0.5 to 1% improvement in thrust specific fuel consumption (TSFC) can be achieved (based on Ref. 1). This translates into roughly a 10^6-bbl/yr fuel savings for wide-bodied jets in this country alone.

Present-day metallic seal systems are limited to temperatures of about 1366 K (2000°F) and require cooling air to maintain them within material operating capabilities. This cooling air is bled from the compressor section and results in some lost performance as high-pressure air is removed from the cycle. With increased turbine gas temperatures, the metallic high-pressure turbine seals may require as much as 4% total engine air for cooling purposes. Clearly, substantial benefits would arise if materials with a high-temperature capability were employed in the high-pressure turbine outer gas path seal location.

One proposed form of improved turbine first-stage outer gas path seal is a plasma-sprayed, layered zirconia/CoCrAlY system on a metallic substrate.[2] Such a seal is designed to have a temperature capability of about 1589 K (2400°F) enabling projected turbine inlet temperatures of around 1811 K (2800°F) to be accommodated. As well as having an improved temperature capability and allowing a reduction in the required cooling air, the proposed seal has another important advantage in its rub-tolerant (abradable) nature. This will result in reduced rotor wear during blade and seal contacts. Rub tolerance of the plasma-sprayed zirconium oxide is due in part to the porous nature of the material, with most of the rub effects being accommodated by wear to the ceramic under some rub interaction conditions. In addition, being an oxide ceramic, greater oxidation and erosion resistance compared to metallic systems would be realized in the gas path seal application. Thus it should be possible to maintain a tighter clearance between the turbine first-stage blade tips and seal, hence improving the turbine efficiency.

There are a number of requirements to be met by the suggested seal system. These include satisfactory performance as regards oxidation and corrosion resistance, abradability, hot gas and particulate erosion resistance, and of course, the obvious need to maintain structural integrity. The purpose of the work described in the present paper was to investigate the latter aspect. The study involved finite element analyses of a particular seal geometry to determine stress and distortion patterns likely to be encountered during steady-state and transient engine operating conditions. The analyses are intended to compliment experimental testing of the seal, which is somewhat smaller in size than will be required for full-scale engine use.[2] Some details of the experimental behavior of the seal during thermal fatigue testing will be presented in the next section.

The Engineering Problem

A cross section of the gas path seal studied is shown in Fig. 2. For the purposes of the current investigation the seal geometry was not varied. The upper or top layer of the seal is comprised entirely of the ceramic zirconia, stabilized with

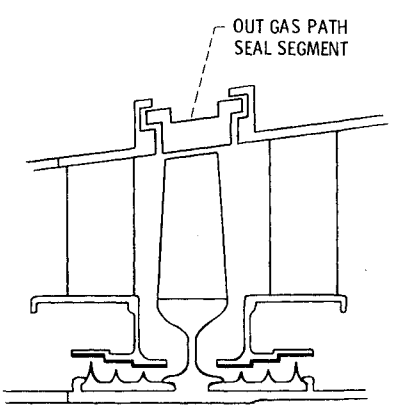

Fig. 1 High-pressure turbine outer gas path seal.

Presented as Paper 78-93 at the AIAA 16th Aerospace Sciences Meeting, Huntsville, Ala., Jan. 16-18, 1978; submitted Feb. 3, 1978; revision received Oct. 19, 1978.

Index categories: Thermal Stresses; Structural Materials.

*Lecturer in Mechanical Engineering, University of Leeds, England.

†Propulsion Laboratory, U.S. Army R&T Laboratories (AVRADCOM).

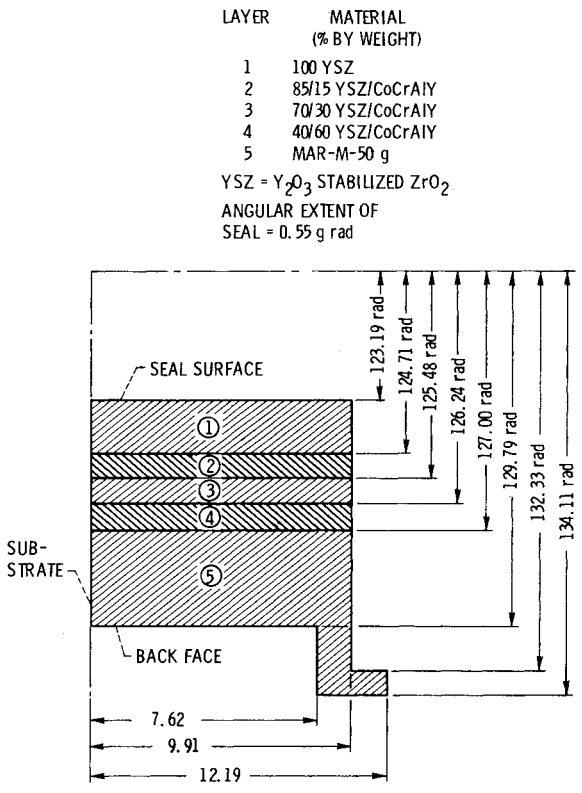

Fig. 2 Cross section of outer gas path seal (units, mm).

yttria. It is the surface of this upper layer that is in contact with the hot turbine gases. Successive layers have a decreasing zirconia content, there being four layers in total sprayed onto the substrate material. Thus a stepwise gradation of material composition is provided, from fully ceramic at the gas path surface to a fully metallic substrate.

The substrate is provided with retaining feet to locate the seal in guideways on the engine casing and is comprised of a cobalt-based super alloy (MAR-M-509). A NiCrAl coat about 0.1 mm (0.004 in.) in thickness is used to improve the bonding of the ceramic system to the substrate, but this has not been modeled in the analysis.

The physical and mechanical properties of the seal materials are shown in Table 1. Many of these properties have been determined specifically in relation to the program of improving gas path seal technology.[2] These properties were used in the analyses performed, a linear variation being taken between the stated temperatures and for reasonable extrapolations outside the ranges given. Where properties were unknown, reasoned guesses have been made.

During the operation of an aircraft gas turbine engine, the outer gas path seal will experience varying temperature conditions. The possibility of fatigue due to cyclic thermal stressing (sometimes known as thermal shock) must therefore be examined. Some results from an experimental program to investigate this are already available.[2] The most significant aspect of the experimental observations was the development of a network of "mud flat" surface cracks consisting of interconnecting circumferential and axial cracks growing in the radial direction. This is consistent with the development of high tensile stresses on the ceramic surface sometime during the imposed thermal cycle. Specimen-to-specimen differences in the number of cycles required to develop the cracks to a significant radial depth have been tentatively identified with microstructural differences from one batch of test seals to another.

Metallographic sectioning revealed laminar (parallel to the seal surface) cracking in addition to the radially growing axial and circumferential cracks. These laminar cracks are observed at or near the interface between the ceramic layer and the first intermediate graded layer. It appears that there may be two mechanisms of origin for the laminar cracks since two distinct types are observed. In some cases the radially growing cracks, driven by the axial and circumferential stresses, seem to turn as they approach the interface, then propagate as laminar cracks. Other laminar cracks apparently initiate independently near the edges of the seal test specimens. The initiation of these latter cracks could be partially due to significant radial tensile stresses at the seal edges.

The purpose of the work described here was to develop analytical approaches to determine distortion and stress patterns that develop in the seal during transient operating conditions and it is hoped, to relate the stress conditions to the observed experimental seal behavior. This capability would enable performance improvements due to, for example, changes in the geometric arrangement and composition of the intermediate layers to be investigated analytically.

For the transient thermal analyis the temperature of the turbine gases at the seal surface and the cooling air fed from the compressor to the substrate back were simulated, as

Table 1 Material, physical, and mechanical properties

	YSZ[a]		85YSZ/15CoCrAlY		70YSZ/30CoCrAlY		40YSZ/60CoCrAlY		MAR-M-509	
Property	Test temperature, K	Property value	Test temperature, K	Property value	Test temperature, K	Property value	Test temperature, K	Property value	Test temperature, K	Property value
Density, kg/m^3	All	4290	All	4982	All	5674	All	7031	All	8858
Poisson's ratio	All	0.25	All	0.26	All	0.27	All	0.28	All	0.30
Young's modulus,	294	46.9	294	25.4	294	36.2	294	58.6	700	197
GN/m^2	1589	15.6	1144	18.6	1061	47.0	1005	92.4	1144	155
Modulus of rupture,	294	28.2	294	41.4	294	56.3	294	223	700	276
MN/m^2	1589	22.9	1144	47.0	1061	70.3	1005	108	1144	276
Coefficient of	294	7.38	294	6.12	294	6.30	294	6.84	700	14.4
expansion, $K^{-1}(\times 10^6)$	1589	8.64	1144	11.0	1061	11.3	1005	12.2	1144	17.1
Specific heat,	476	550	476	534	476	516	476	483	476	445
J/kg K	1366	646	1366	643	1366	638	1366	625	1366	609
Thermal conductivity,	366	0.51	366	0.51	366	0.51	366	0.51	—	—
W/m K	533	0.51	533	0.58	533	0.62	533	0.67	—	—
	811	0.54	811	0.78	811	0.93	811	1.04	—	—
	1089	0.59	1089	1.06	1089	1.32	1089	1.52	—	—
	1366	0.71	1366	1.45	1366	1.85	1366	2.20	—	—
	1644	1.01	1644	2.03	1644	2.61	1644	3.18	1644	52.7

[a] Y_2O_3-stabilized ZrO_2.

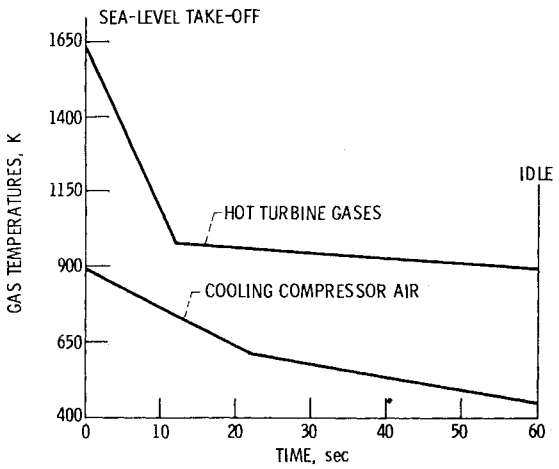

Fig. 3 Assumed gas temperature variations from sea-level takeoff to idle condition.

shown in Fig. 3. The temperatures are representative of those in an engine decelerated from sea-level takeoff to idle conditions in a period of 1 min and have been estimated from seal surface and back face temperatures.[2] The stress conditions to which the seal is subjected during the deceleration cycle have been identified as being important in its thermal shock performance.

Analysis

The computer programs used to generate the results presented in this paper were made available through the Computer Services Division of the National Aeronautics and Space Administration's Lewis Research Center and were operated on the Center's UNIVAC 1100 computer.

Transient Thermal Analysis

The SINDA (systems improved numerical differencing analyzer) code was used to generate transient temperature profiles throughout the seal during the deceleration cycle. This program enables analysis of thermal systems represented in electrical analog, lumped-parameter form. Axisymmetric thermal conditions were taken to apply. Indeed since the axial extremities of the seal were taken to be insulated (as no detailed information on thermal conditions there was available), the seal temperatures turn out to be effectively a function only of the radial coordinate and, of course, time.

Stress Analysis

Thermal stresses in the seal were estimated using two finite element programs, one being a two-dimensional stress analysis program, the other having the capability of dealing with three-dimensional geometries. By using the two codes it was hoped to learn how appropriate the use of the simple two-dimensional analyses were in terms of satisfactory prediction of stresses in the seal. The two-dimensional code employed was the FEATAGS (finite element analysis temperature and general stress) program. This code can deal with axisymmetric or plane bodies. The temperature data generated by the SINDA program were used as input to the two-dimensional stress code providing the thermal loading for the seal at specified time intervals during the engine deceleration cycle. The program can also undertake steady-state thermal analyses and was used to check the temperature patterns predicted by the SINDA code for the sea-level takeoff steady-state conditions. Excellent agreement was found.

For three-dimensional stress analysis of the seal, the MARC (Marc Analysis Research Corporation) program was used. Temperature profiles generated by the SINDA code (and taken to be a function of radius only) were again used as the thermal loading input. In due course the capability of the MARC code to undertake the transient thermal analysis will be employed.

All analyses carried out with the stress codes assumed that the seal was free to distort as it required. That is, no boundary restrictions on its movement, even at the mounting feet locating it to the engine casing, were applied. As will be seen, the structural integrity of the seal is challenged even if it is allowed to expand freely. Computations, details of which will not be presented here, have indicated that if the seal is restrained at the mounting feet, the enhancement of the thermal stresses it sees are such as to suggest that material failure in some form would be inevitable.

All calculations performed with the stress codes assumed that the materials of the seal behaved elastically, even if stresses greater than those required for yielding or crack initiation were attained. The extension of the analyses to deal with plastic material behavior is a possibility with the programs. The primary interest in the work was to obtain a measure of the stress variations in the seal, and hence details of the distortions that have also been determined will not be presented here.

Results and Discussion

Temperature Distributions

In determining the temperature profiles shown in Fig. 3, the following heat transfer coefficients were used at the seal surface and back face, respectively: 5700 and 11,400 W/m^2 K (1000 and 2000 Btu/h ft^2 °F). The film coefficient used for the back face (11,400 W/m^2 K) is estimated from impingement cooling measurements for various turbine cooling schemes.[3] For the seal surface, the value of 5700 W/m^2 K is considerably higher than calculated values for turbulent flow over a flat plate.[4] The high value selected for the seal surface partly reflects impingement effects attributable to blade sweep. Temperature distributions on the axial line of symmetry are shown. The distributions are for sea-level takeoff and idle (60 s into the deceleration cycle but not quite steady state) conditions, together with profiles at 6, 12, and 20 s into the cycle.

It is immediately noticeable that during the transient variation of temperature between sea-level takeoff and idle conditions, the situation may arise in which the seal temperature maximizes below the surface. Such situations reflect the convection of heat from the seal surface to the turbine gases as the surface temperature exceeds that of the gases, which has fallen rapidly. Despite the fact that the temperature

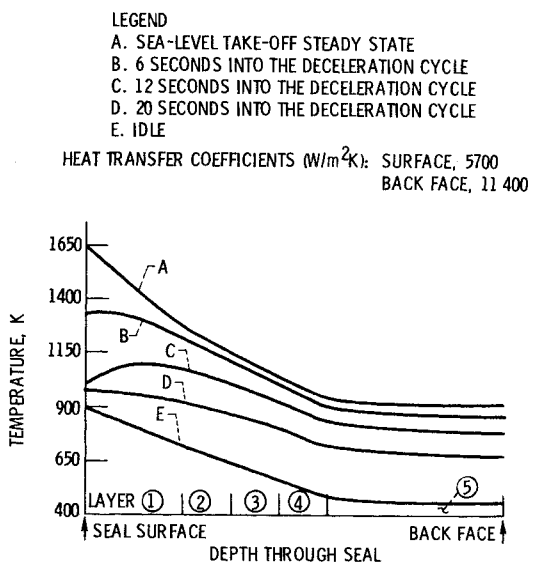

Fig. 4 Transient temperature profiles through the seal on the axial line of symmetry.

of the seal at a time 12 s into the deceleration cycle is much less than at the steady-state sea-level takeoff condition, the stressing of the seal may be more severe due to the temperature maximizing below the surface. For example, the possibility of subjecting the surface layer to tensile stresses becomes apparent. Figure 4 also illustrates how well the top four layers of the seal protect the substrate from high temperatures. The temperature drop across the substrate is very small due to its relatively high thermal conductivity.

The surface heat transfer coefficients that have been used in the determination of the temperature profiles shown in Fig. 4 are by no means precisely known parameters. The temperature profiles of Fig. 4 have, in the main, been used to determine seal stress distributions presented later. However, a brief examination of the effect of varying the heat transfer coefficients has been undertaken.

In Fig. 5 the temperature profiles A, C, and E of Fig. 4 are compared with profiles obtained using alternative heat transfer coefficients. The heat transfer coefficients already designated are termed case 1. For case 2 the heat transfer coefficient at the seal surface was reduced by a factor of 10, the intention being to reflect a reduced heat transfer capability appropriate at the less turbulent gas flow conditions near engine idle. In addition, for case 3 it was assumed that the seal surfaces took up the temperature of the gases with which they were in contact.

It can be seen from Fig. 5 that the conditions of case 3 have only a minor effect on the temperature profiles compared with case 1. However, reducing the heat transfer coefficient by an order of magnitude at the hot surface has a noticeable, and expected, effect on the top surface temperatures at the sea-level takeoff and idle conditions.

Stress Distributions

Before giving details of the stresses developed in the seal, it is necessary to clarify certain aspects of the finite element analyses and the manner in which the results are presented.

In the three-dimensional analysis, because of the prevailing symmetry, it was only necessary to consider one quarter of the seal. The portion taken is shown in Figs. 6-8, there being two views in order to present axial and circumferential stresses. The centerlines of the views pass through the midpoint of the seal surface. It will be noted that the views are not scaled, the half-length of the seal being in fact three and one-half times the half-width and five times the depth. In addition, the circumferential curvature of the seal has not been depicted although it was considered in the analysis.

With the two-dimensional analysis of the seal, both axisymmetric and axial plane stress conditions were

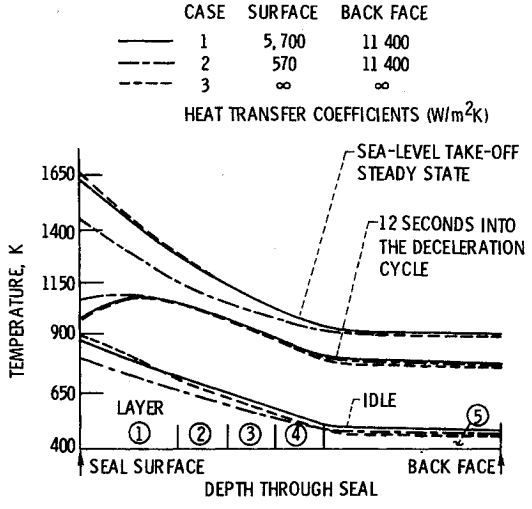

Fig. 5 Temperature profiles through the seal on the axial line of symmetry for varying heat transfer coefficients.

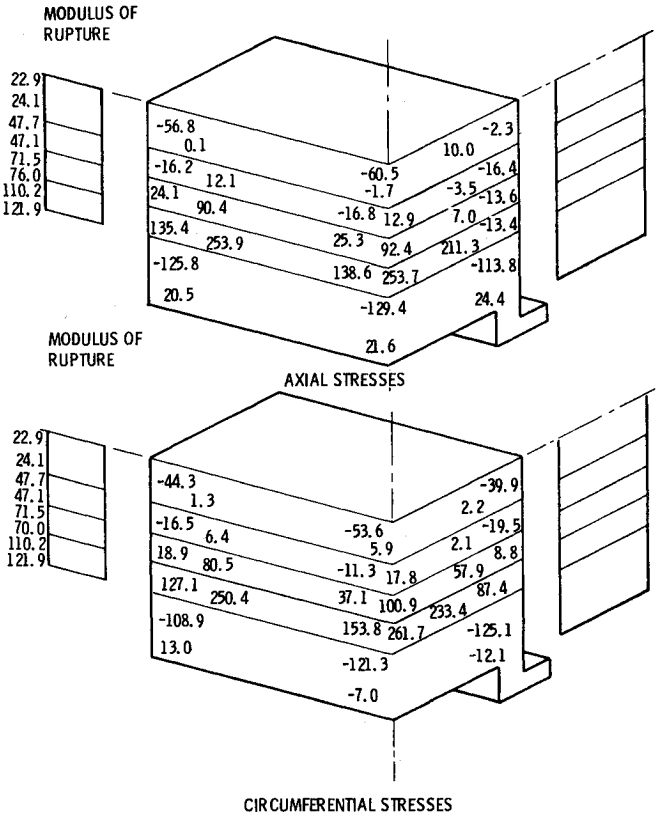

Fig. 6 Axial and circumferential stresses in outer gas path seal—sea-level takeoff steady state (three-dimensional analysis; units, MN/m²; tensile + ve).

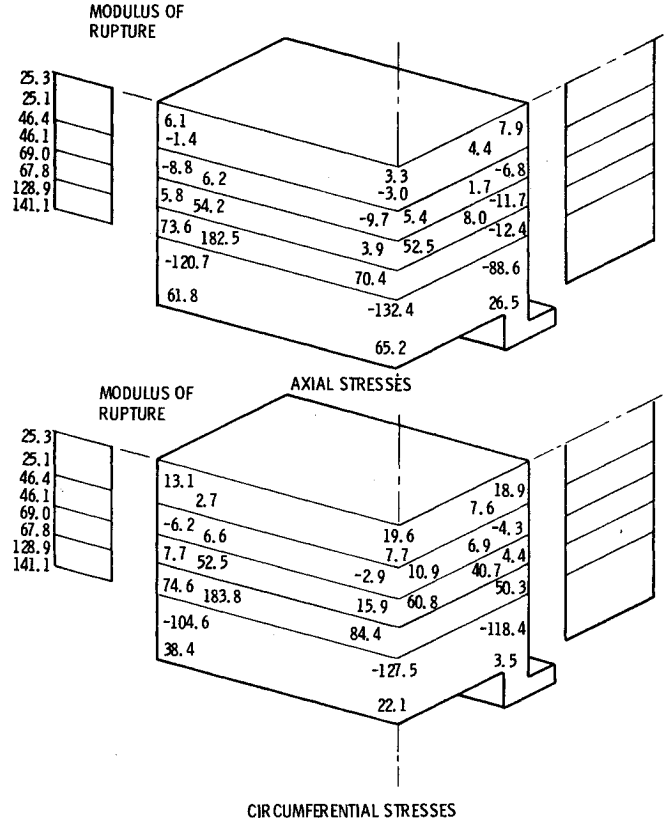

Fig. 7 Axial and circumferential stresses in outer gas path seal—12 s into the deceleration cycle (three-dimensional analysis; units, MN/m²; tensile + ve).

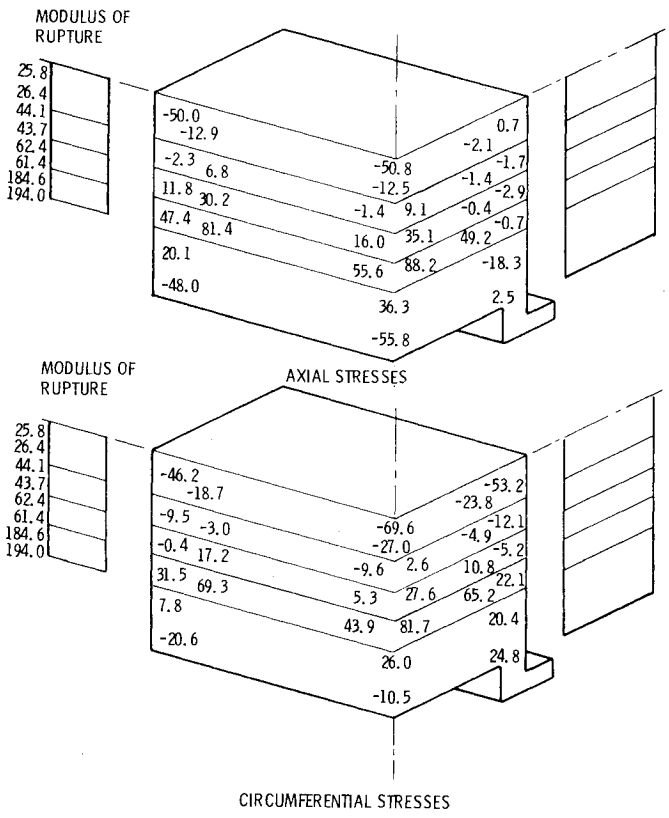

Fig. 8 Axial and circumferential stresses in outer gas path seal—idle (three-dimensional analysis; units, MN/m^2; tensile + ve).

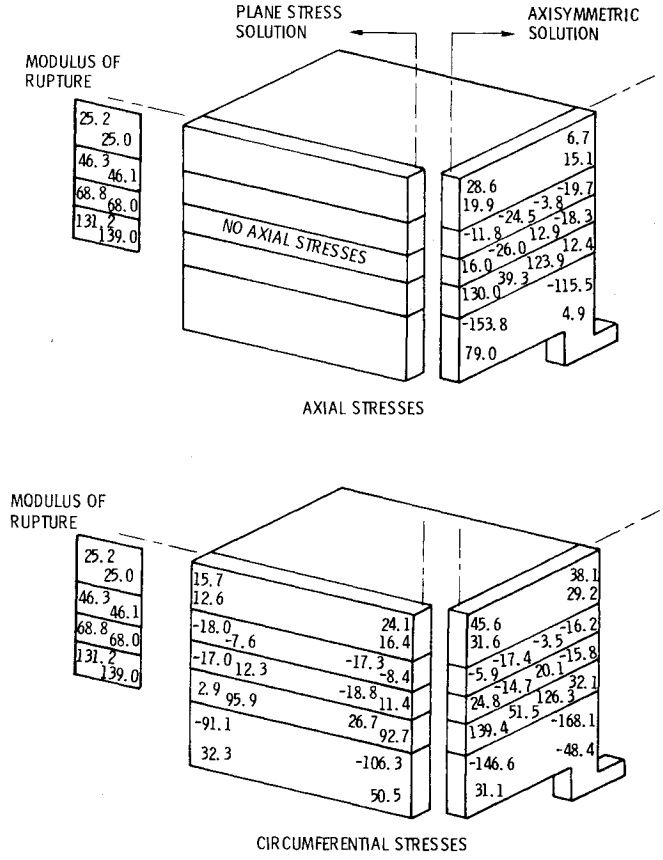

Fig. 10 Axial and circumferential stresses in outer gas path seal—12 s into the deceleration cycle (two-dimensional analysis; units MN/m^2; tensile + ve).

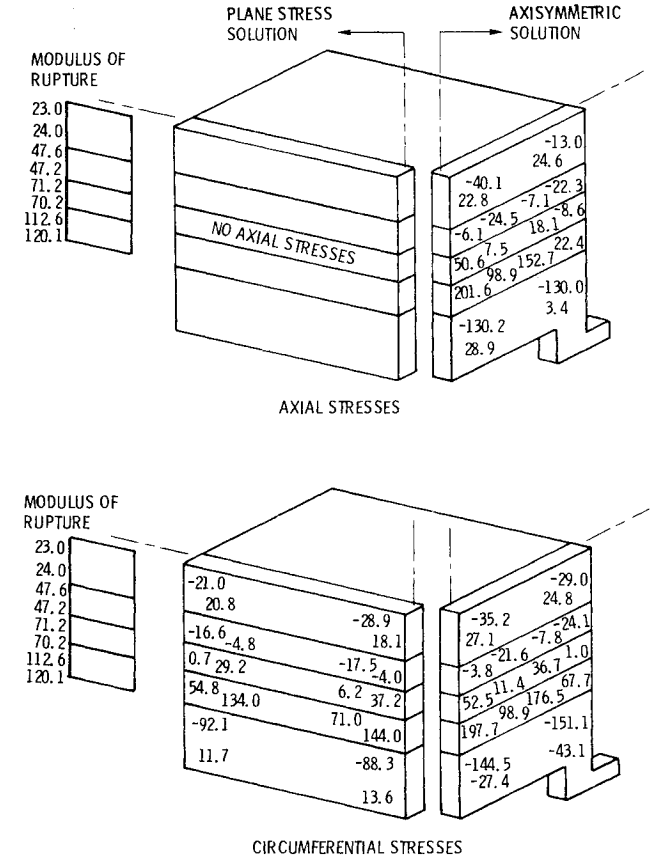

Fig. 9 Axial and circumferential stresses in outer gas path seal—sea-level takeoff steady state (two-dimensional analysis; units, MN/m^2; tensile + ve).

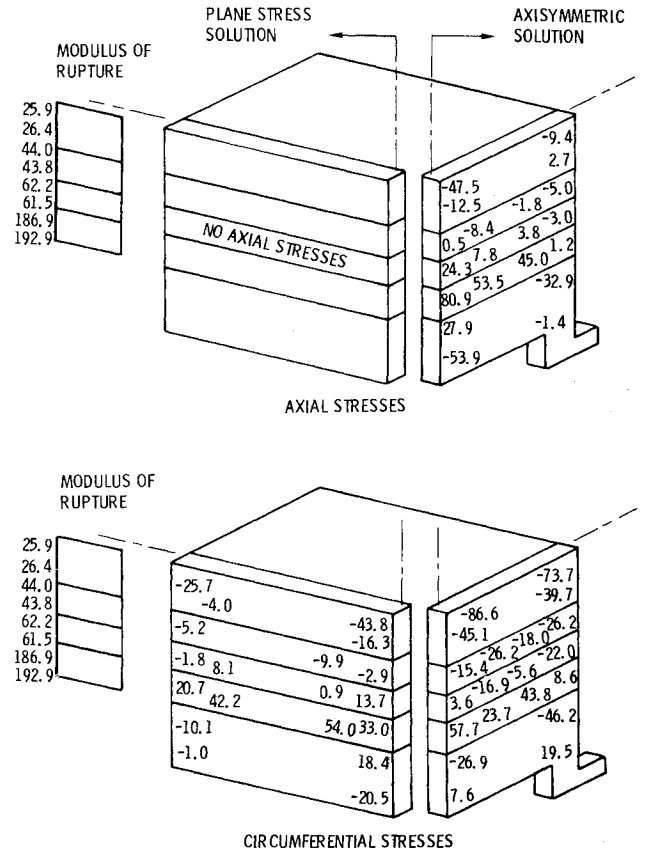

Fig. 11 Axial and circumferential stresses in outer gas path seal—idle (two-dimensional analysis; units, MN/m^2; tensile + ve).

examined. For the plane stress analysis curvature effects were neglected. A typical form of presentation of the calculated stresses is shown in Figs. 9-11. Data are given on central planes circumferentially and axially. In this way, easy comparison with the three-dimensional analysis is possible, the latter being very nearly on central planes.

It is not our intent to describe the details of the finite element structures adopted to model the seal geometry. Neither will the precise spatial positions at which stress values are presented be given, since it is intended only to give an overall feel for magnitudes and the approximate location. In broad terms the stresses are given at points close to the interfaces concerned and close to the extremities of the sections considered. The positions at which stress values are given are similar for the two- and three-dimensional analyses.

Only details of axial and circumferential stresses are presented. Radial and shear stresses are, in general, small in comparison, particularly in the interior of the seal. At the axial and circumferential extremities this is not always the case, and this may have significance in the origin of one mode of laminar crack mentioned previously. Since the radial and shear stresses are small, it follows that the axial and circumferential stresses presented are very often effectively principal stresses. The stress values are given in terms of a Cartesian coordinate system constructed on the diagrams' centerlines.

Details of the stress results will now be presented. It should be emphasized that it has been assumed that the seal is in a stress-free state at ambient temperature conditions, 297 K (70°F) (i.e., residual stresses are neglected). In Figs. 6-8 stress distributions (from the three-dimensional analysis) corresponding to the temperature distributions at sea-level takeoff (A), 12 s into the deceleration cycle (C), and idle (E) of Fig. 4 are shown. The modulus of rupture at the locations where the stress results are given are shown for the four ceramic containing layers. The following major points are worthy of note:

1) At sea-level takeoff conditions (Fig. 6), the top layer of the seal is subjected to sizeable compressive stresses. The fourth layer, which is bonded to the substrate, is in considerable tension with the modulus of rupture having been exceeded in the elastic analysis. Thus it is probable that yielding of the material of the fourth layer would occur, resulting in some stress relaxation.

2) Twelve seconds into the deceleration cycle (Fig. 7) the fourth ceramic layer is still in considerable tension. The top layer is also subject to tensile stresses now, although these are predicted not to exceed the modulus of rupture.

3) At idle conditions (Fig. 8) the top layer of the seal is once again predicted to be heavily in compression.

The performance of the zirconia/CoCrAlY layers would be expected to be far better under compression than when in tension. Thus a conclusion from the aforementioned results might be that apart from the high tensile stresses in the 40 zirconia/60 CoCrAlY layer, the possibility of the seal remaining structurally intact during thermal cycling appears to be reasonable. However, it must be recalled that it has been assumed that the seal is in a stress-free state at ambient temperature conditions. Its method of manufacture is such as to result in residual tensile stresses in the surface layer. Experimental determination of the residual stress distribution[2] has indicated that the tensile stress at the seal surface at ambient conditions is of the order 20.7 MN/m^2 (3000 psi). If tensile stresses of this order of magnitude are superimposed on those predicted in the top layer of the seal at a time 12 s into the deceleration cycle, it can be seen that the modulus of rupture is exceeded. Indeed the analytical results become consistent with the experimentally observed surface cracking. A catastrophic structural failure would not be expected at a low number of thermal cycles, and indeed this is not the case experimentally.

Figures 9-11 show stress distributions calculated by the two-dimensional analyses for the same conditions as Figs. 6, 7, and 8, respectively. The results are presented mainly for comparison with the three-dimensional-analysis results and to assist in the realistic interpretation of the results of future two-dimensional analyses should the latter prove appropriate. It is apparent that the trends of the calculated stresses of Figs. 9-11 bear comparisons with the three-dimensional analysis results. It is also particularly noticeable that at a time 12 s into the deceleration cycle, the two-dimensional analyses predict greater tensile stresses in the surface layer.

Alternative Surface Heat Transfer Coefficients

In Fig. 5 the effect of two alternative combinations of boundary heat transfer coefficients on the temperature profiles from Fig. 4 are shown. Two-dimensional failure element computer program calculations have indicated that the difference in temperature distributions would cause relatively small differences in stress patterns. An examination of Fig. 4 adds weight to this conclusion, particularly when it is observed that the temperature distributions at 12 s into the cycle and at idle conditions do not vary much. The most obvious effect on the stress distributions was predicted at steady-state sea-level takeoff conditions; here the circumferential stresses in the top layer near the interface with the second layer were somewhat more tensile for case 2 of Fig. 5 than for the other two cases.

It is concluded that the lack of precise heat transfer coefficients may not be a significant drawback in analytical attempts to predict seal configurations with improved thermal shock behavior.

Alternative Variation of Compressor Cooling Air Temperature

The assumed variations in gas temperatures were assessed from calculated engine seal segment temperature cycles. The

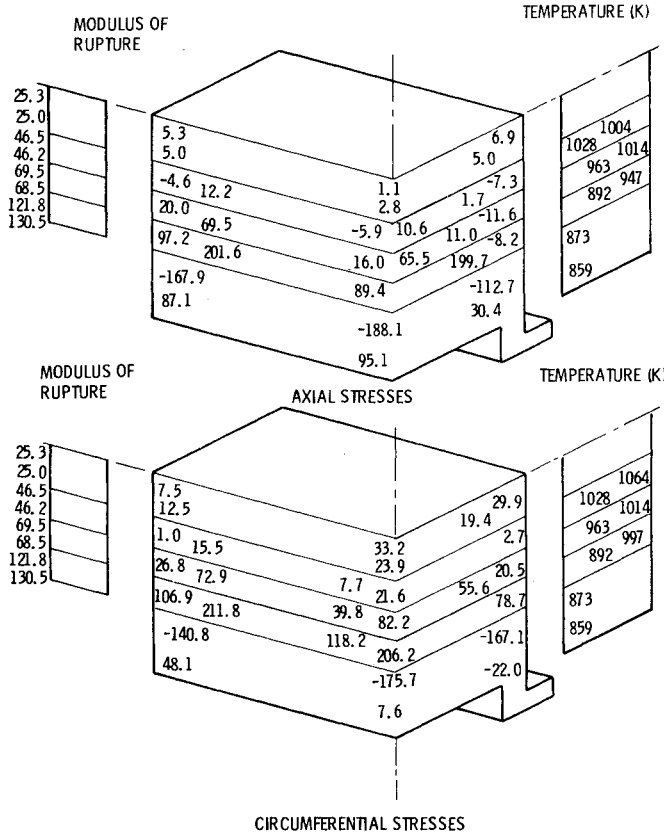

Fig. 12 Axial and circumferential stresses in outer gas path seal with alternative compressor cooling air temperature—12 s into the deceleration cycle (three-dimensional analysis; units, MN/m^2; tensile + vr).

test specimens have, however, been subjected to a slightly different thermal cycle during fatigue testing.[2] In particular the temperature of the back face of the metallic substrate fell to only about 616 K (650°F) at idle simulation rather than the 950 K (350°F) indicated in Fig. 2. Such a difference could be significant. The higher back surface temperature might cause more pronounced maximizing of the seal temperature below the surface and possibly more adverse (tensile) stressing in the ceramic.

To investigate this, it was assumed that the compression cooling air temperature varied linearly from 894 K (1150°F) to 616 K (650°F) during the 60-s deceleration cycle. The hot turbine gases were taken to vary as shown in Fig. 3. At sea-level takeoff steady-state conditions, the temperature and stress distributions are the same as presented already. At 12 s into the cycle temperature and stress profiles were calculated to be as shown in Fig. 12.

The surface and maximum seal temperatures were, respectively, 1010 K (1359°F) and 1084 K (1492°F) compared to 987 K (1317°F) and 1020 K (1377°F) for case C of Fig. 4. As can be seen by comparing Figs. 6 and 11, significantly higher circumferential stresses are predicted to occur in the top ceramic layer with the higher back face cooling air temperature. The predicted stress pattern is, however, still consistent with the available thermal fatigue experimental evidence.

Relief of Surface Tensile Stresses

Both the results of the analyses presented here and the experimental testing suggest that tensile stresses comparable to the strength of the ceramic material occur in the ceramic layer during the deceleration cycle. Consideration is given to two schemes whereby these tensile stresses could be reduced.

In the first scheme, a bending moment is applied to the metallic substrate before spraying the metal/ceramic and ceramic layers. The sense of the bending moment would be such as to compress the ceramic layer of the seal on release of the moment after spraying. So that no yielding would occur during the thermal cycle, the bending stress in the substrate should not exceed 276 MN/m^2 (40,000 psi). The maximum allowable bending moment would then be about 360-MN/m width (about 9-ft-lb/in. width). Upon release of this bending moment after spraying, residual compressive stresses in the ceramic top layer are estimated to be about 13 MN/m^2 (1900 psi). Such a magnitude of stress is significant compared to the circumferential surface stress in the ceramic top layer shown in Fig. 7, and might be expected to contribute to the life of the seal.

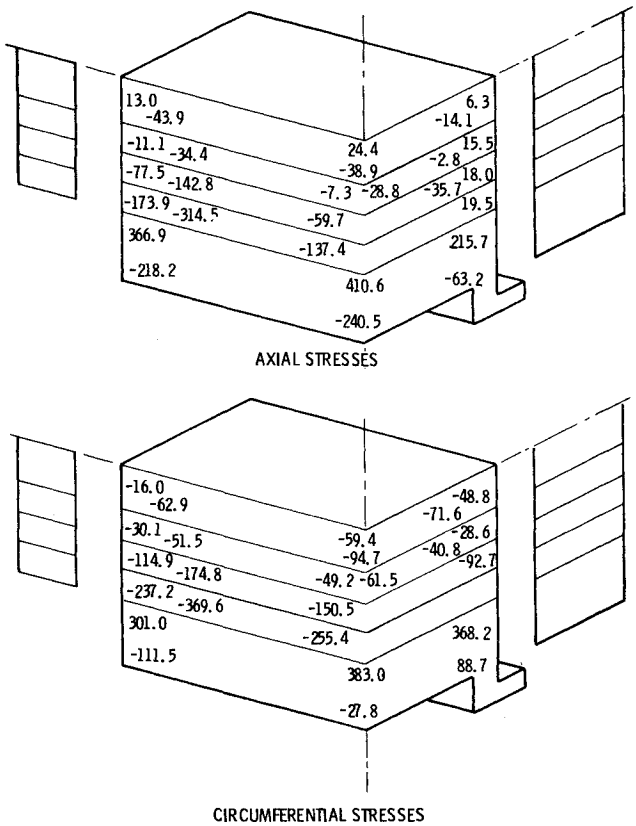

Fig. 13 Stresses in outer gas path seal at 294 K, assuming stress-free condition at 1366 K and elastic behavior (units, MN/m^2).

Another potential approach to the relief of surface tensile stresses in the ceramic is to subject the seal system to an annealing process, or to fabricate the seal at an elevated temperature so that a stress-free temperature would result. By way of example, consider a 1366 K (2000°F) annealing process whereby all residual stresses are relaxed out of the seal system. Upon cooling to room temperature a new residual stress pattern is developed, as summarized in Fig. 13. Of special importance are the compressive circumferential stresses in the ceramic top layer. It would appear that the high-temperature annealing approach has a promising potential in regard to providing a favorable prestress to the seal system. An unresolved question, however, is the significance of the tensile residual stresses in the axial direction in the topmost portion of the ceramic layer. These tensile stresses are quite high, although in the axial direction the bulk of the ceramic layer is under compressive axial stress.

Concluding Remarks

The stress patterns determined analytically during the deceleration cycle are consistent with observed experimental thermal shock behavior of the test seal. This gives some confidence in applying the programs in parametric studies to attempt to improve the seal configuration. The following aspects merit attention in future studies:

1) The determination of a representative axial variation in temperature in the seal and its importance to stresses developed.

2) An optimization of relative layer depths in the seal. The results presented in this paper suggest that the minimization of the tensile stresses in the top ceramic layer would be a suitable criterion for the optimization process.

3) A study of an actual engine seal geometry. The larger size seal which will be used in practice (probably with different aspect ratios to the test seal) may exhibit characteristics not predicted by analysis of the smaller seal.

Summary of Results

1) The magnitude of the surface heat transfer coefficients used in the analysis does not appear to be highly sufficient.

2) Transient temperature distributions in the gas path seal show a maximum below the surface. This tends to cause tensile strength in the top ceramic layer.

3) Stress analysis of the seal using two-dimensional finite element programs predicts trends consistent with the three-dimensional analysis results. It is expected that two-dimensional stress analysis would be useful in early parametric studies to improve the seal configuration.

4) The magnitude of the thermal stresses determined, taking account of residual stresses known to be present, suggests that the top layer of the seal suffers tensile stresses exceeding the modulus of rupture. This is also true of the fourth (40 zirconia/60 CoCrAlY) layer.

5) Radial and shear stresses developed in the seal are, in general, negligibly small. However, this is not always true at the seal edges, and this may have significance in the development of some laminar cracks.

6) Computations have indicated that since the seal is not free to distort without restriction, its stressing will be such as to lead almost inevitably to material failure.

Acknowledgment

C. Taylor was in receipt of a National Research Council Senior Research Associateship during the period when the work described in this paper was carried out.

References

[1] Glassman, A. J., ed., "Turbine Design and Application," Vol. 2, NASA SP-290, 1973, p. 125.

[2] Shiembob, L. T., "Development of a Plasma Sprayed Ceramic Gas Path Seal for High Pressure Turbine Applications," NASA CR-135183, May 1977.

[3] Liebert, C. H. and Stepka, F. S., "Potential Use of Ceramic Coating as a Thermal Insulation on Cooled Turbine Hardware," NASA TM X-3352, Feb. 1976.

[4] Rohsenow, W. M. and Choi, H. Y., *Heat, Mass and Momentum Transfer*, Prentice Hall, Englewood Cliffs, N.J., 1961.

[5] Taylor, C. M., "Thermal Stress Analysis of a Graded Zirconia/Metal Gas Path Seal System for Aircraft Gas Turbine Engines," NASA TM X-73658, Apr. 1977.